Eutectic Syntheses of Graphitic Carbon with High Pyrazinic Nitrogen Content

Nina Fechler, Niels P. Zussblatt, Regina Rothe, Robert Schlögl, Marc-Georg Willinger, Bradley F. Chmelka, and Markus Antonietti*

Carbon nanoarchitectures, such as fullerenes, nanotubes, and graphenes, are versatile and promising materials whose properties depend essentially on their structures and surface compositions.[1] Standard sustainable precursors for carbon include phenol–formaldehyde resins,[2–5] carbohydrates, or even crude biomass, though the use of such precursors reduces control over composition.[6,7] From a synthesis perspective, a significant processing advantage can be realized by applying liquid precursors with little or no volatility, including ionic liquids [8–10] or deep eutectic mixtures.[11] Due to the fluidity, shaping and/or coating processes are simple, as is the use of structure-directing agents, chosen based on polarity and miscibility with the liquid precursor, to introduce defined porosity. As a desirable secondary effect, use of liquid precursors allows convenient syntheses of carbonaceous nanostructures with controlled contents of nitrogen,[12] phosphorous,[13] boron, [14] and/or sulfur-dopants [15] with useful properties, including high oxidation stabilities ("noble carbons"), high conductivities, and various degrees of (electro)catalytic activities.[16,17] The reason for these improved properties is still disputed,[18,19] but the role of local electron density and heteroatom distribution within the designed carbon nanoarchitectonics appears to be of key importance.[20–22] However, understanding and control of the local material composition and structure on the level of atomistic element patterns and their regularity has been difficult to achieve due to the inherently dynamic and random nature of current carbon syntheses.

Here, a new synthesis approach is presented based on supramolecularly preorganized precursor mixtures composed of phenols/ketones and urea, which combine the processability and homogeneity of liquids with the well-defined structure of prealigned liquid crystals. This is in contrast to other works using DES for carbon synthesis mainly leading to isotropic mixtures and carbons of comparably low nitrogen content.[23,24] Phenols and ketones are a multifarious group of readily available, structurally flexible, and inexpensive chemicals which are also a significant product of proposed biorefinery schemes[25–28] while simple urea serves as an effective nitrogen source and melting point reduction agent. Due to strong hydrogen-bonding, these monomers form deep eutectic liquid mixtures that are well-suited for liquid-based carbon synthesis. In addition, it is possible to choose among various phenol/ketone precursors to control the initial orientation and degree of cocondensation of the final material in a "mosaic-like" approach to control the nanoarchitecture. As a result, control over preorganization, functionality, and heteroatom-doping in the target carbon material can be accomplished in a comparably simple and modular fashion, i.e., we intend to follow a concept of "nanoarchitectonics for mesoporous materials."[29]

The central objective lies in attaining improved chemical control over the entirety of the condensation process. This requires liquidity/plasticity in the first reaction stages, along with adjustable wettability and the coupled possibility of coating or templating. This has to proceed to the preorientation of the to-be-formed graphitic materials, here via supramolecular/liquid-crystalline precondensates. This work seeks to bring pyrolysis (also referred to as "carbonization" or "coalification"), with its rather challenging to understand processes and poor control and reproducibility, closer to concepts such as polycondensation (known from polymers) with improved reaction control. We especially focus in this paper on the condensation of urea with cyclohexanhexone, a precursor without any C—H—bonds. The different reaction steps and the resulting materials are characterized by X-ray diffraction (XRD), nuclear magnetic resonance (NMR) spectroscopy, elemental analysis, high-resolution electron microscopy, electron energy loss spectroscopy (EELS), and X-ray photoelectron spectroscopy (XPS). Combined understanding from these techniques indicates a covalently bound, highly aromatic carbon/nitrogen-material with the approximate composition of C_2N, high homogeneity, and the nitrogen predominantly present as pyrazinic units. An idealized scheme of this reaction is presented in **Scheme 1**.

The ability of three representative phenols/ketones to form eutectic mixtures with urea was explored, though restricted to stoichiometric compositions allowing further condensation (i.e., two hydroxyl- and/or oxo-groups per two nitrogen moieties present in urea). By choice of the monomer (**Table 1**), a range

Dr. N. Fechler, R. Rothe, Prof. M. Antonietti
Max Planck Institute of Colloids and Interfaces
Department of Colloid Chemistry
Research Campus Golm
14424 Potsdam, Germany
E-mail: nina.fechler@mpikg.mpg.de
N. P. Zussblatt, Prof. B. F. Chmelka
Department of Chemical Engineering
University of California at Santa Barbara
Santa Barbara
CA 93106, USA
Prof. R. Schlögl, M.-G. Willinger
Fritz Haber Institute of the Max Planck Society
Department of Inorganic Chemistry
Faradayweg, 4-6, 14195 Berlin, Germany
Dr. M.-G. Willinger
Max Planck Institute for Chemical Energy Conversion
Department of Heterogeneous Reactions
Stiftstrasse 34-36, 45470 Mülheim an der Ruhr, Germany

DOI: 10.1002/adma.201501503

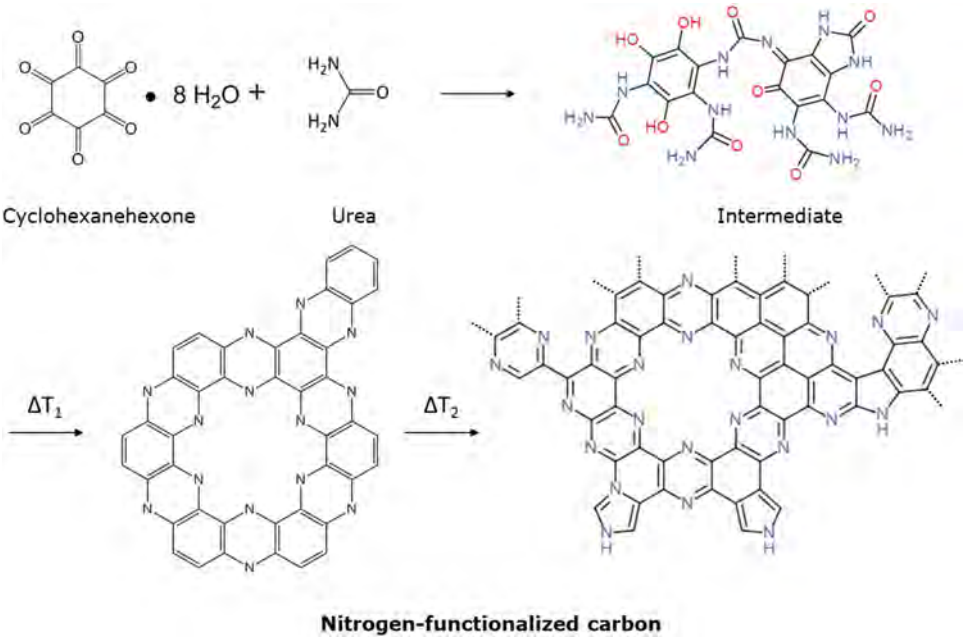

Scheme 1. Depiction of synthesis process of cyclohexanehexone and urea reactants to a cross-linked intermediate material (top), which at temperatures in excess of 500 °C ($T_1 < T_2$), converts stepwise to nitrogen functionalized carbons containing primarily pyridinic and pyrazinic nitrogens (bottom).

of aggregation architectures was investigated. These included locally interacting, "0D"- stacked discotic entities produced with 1,2-benzoquinone (SCM-2-*y*), "1D", linear aggregated, polymeric materials synthesized with 2,5-dihydroxy-1,4-benzoquinone (SCM-4-*y*), and "2D"-extended aggregation networks from cyclohexanehexone (SCM-6-*y*). Note that the precursors cyclohexanehexone and urea do not contain any C—H linkages, which will be shown to simplify the further thermal transformations as the aromatic C—H bond is very strong and thus usually counteracts condensation. Structures of precursors and

Table 1. Precursor ratios, eutectic melting points, and elemental composition following condensation of supramolecular carbonaceous materials at varying temperatures.

Label	Precursor components		Molar mix-ratio	Mix melting point [°C]	Condensation temperature (*y*) [°C]	Elemental composition of SCM [wt%]			
	1	2				N	H	C	C/N
SCM-2-*y*	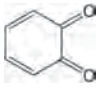 1,2-benzoquinone		1:1	68.5	90	13.0	5.6	49.1	3.1
					500	31.0	2.5	49.0	1.6
					800	12.5	1.3	76.0	6.1
SCM-4-*y*	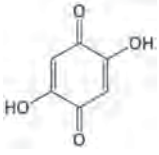 2,5-dihydroxy-1,4-benzoquinone	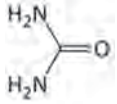	1:2	129	135	22.3	4.3	39.3	1.7
					500	18.0	2.5	64.0	3.5
					800	15.0	1.9	75.0	5.0
SCM-6-*y*	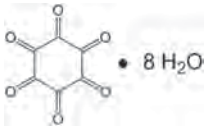 cyclohexanehexone	urea	1:3	68.0	90	22.0	4.0	29.0	1.3
					500	36.0	2.0	52.0	1.4
					800	28.0	1.3	63.0	2.2

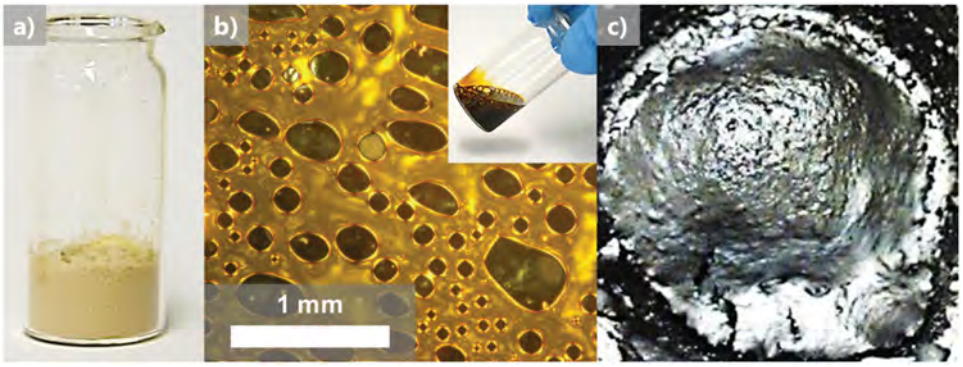

Figure 1. Photographs of the synthesis process: a) powder of the cyclohexanehexone:urea mixture at room temperature. b) Optical microscopy of the liquid-crystalline eutectic mixture in the supercooled liquidus, partial polarization mode (insert: macroscopic view); c) cohesive, silvery reflecting monolithic carbon foam after condensation at 500 °C.

some representative composition data for materials prepared at various condensation temperatures are presented in Table 1. Note that the sum of weight percentages does not equal 100%, which is likely due to the high stability and thus incomplete combustion of the materials. This is also supported by XPS which reveals low oxygen contents for the condensed materials (Table SI-1, Supporting Information, XPS surface composition data).

The diverse phenomenon occurring during synthesis process are representatively shown for the cyclohexanehexone and urea-based materials (SCM-6-*y*) in **Figure 1**a–c. Starting from a powder mixture of cyclohexanehexone and urea (Figure 1a), gentle heating results in liquefaction below the melting point of the respective components (here 68 °C), indicating deep eutectic behavior. Simultaneously, a color change from beige to dark orange is observed (Figure 1b, inset). The eutectic mixture can be easily supercooled and examined by polarization microscopy to show birefringence typical for liquid crystals (Figure 1b). This indicates the development of a stacked, aromatic charge-transfer system, i.e., the coupling of the monomers towards larger, preorganized assemblies. During heating, the evolution of water and gases from monomer condensation or potential some decomposition are observed. Reactivity of the precursor components was noticed to increase with the number of hydroxyl- and/or oxo-groups.

For 1,2-benzoquinone and urea (SCM-2-90), cooling of the eutectic generates a crystalline solid (Figure SI-1d,e, Supporting Information). For 2,5-dihydroxy-1,4-benzoquinone and urea, condensation occurs along with an increase in viscosity similar to cyclohexanehexone-based materials, first forming a sticky plastic state which can be pressed to films or spun to fibers (Figure SI-2, Supporting Information). Finally, these systems adopt a resin-like state which suggests the development of an extended network structure, likely via both covalent linkages and hydrogen-bonds. FT-IR measurements of the sample prepared from cyclohexanehexone and urea at 90 °C show signal shifts compared to the pure educts indicating hydrogen bond interaction of the amine and ketone functionalities (Figure SI-3, Supporting Information). Furthermore, size exclusion chromatography (SEC) measurements in DMSO reveal a molecular mass of 2600 g mol^{-1} for 2,5-dihydroxy-1,4-benzoquinone and in the case of cyclohexanehexone after 1 d dissolution-time, 900 g mol^{-1}, and after 3 d, 470 g mol^{-1}. These findings further hint to strong but reversible hydrogen bonds supporting the results obtained from liquid NMR and XPS. Adjustment of viscosity by addition of water was determined to be a processing option in most cases, though this may influence local order and organization.

Further condensation at 500 °C leads to carbons of varying appearance which again can be related to the various observed modes of preorganization. While the material prepared from 1,2-benzoquinone (SCM-2-500) forms black needles, those synthesized from the other precursors (see SCM-6-500, Figure 1c) are silvery black carbons with pronounced metallic gloss and a cohesive, monolithic foam morphology which is strongest for the cyclohexanehexone-derived materials. It is to be noted that the formation of such "metallic" states following heating to the comparatively low temperature of 500 °C is very unusual, however known from conducting polymers and is regarded as one of the advantages of the described synthesis.

Importantly the elemental compositions of the materials synthesized by condensation at 500 °C are very close to reaction products formally obtained by the removal of all condensable water molecules (i.e., a "$C_{0.6}N_{0.4}$" for the SCM-6-500 species and a "$C_{0.66}N_{0.33}$" for the SCM-4-500 species) indicating that urea and quinones readily condense in a first step via water elimination toward the black–silver polymer resin-like species. Interestingly, the compositions of the materials synthesized by heat treatment at 500 °C are oxygen-poor, even assuming the maximum number of possible dehydration reactions, indicating there is a second oxygen elimination reaction active already at comparably low temperatures.

TGA–MS measurements were performed to support this molecular picture. The only elimination products which could be identified were H_2O followed by CO and N_2 (Figure SI-4, Supporting Information). At temperatures greater than 700 °C, this is followed by combustion processes due to residual oxygen. This product pattern is in agreement with a proposed condensation mechanism eliminating first water, then the excess of urea fragments.

XRD patterns (**Figure 2**) are in good agreement with visual appearances as the diffractograms of the various materials exhibit features indicating the presence of liquid-crystal domains, condensed preorganized polymers prior to heat

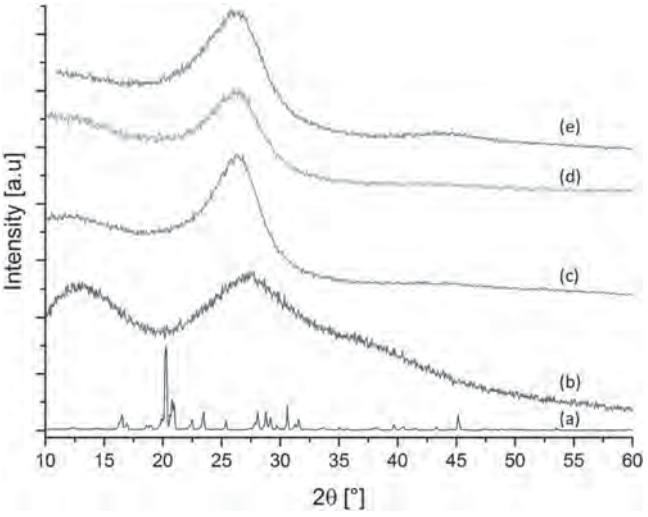

Figure 2. X-ray diffraction patterns of supramolecular carbonaceous materials based on 1,2-benzoquinone/urea and cyclohexanehexone/urea at varying condensation temperatures: a) SCM-2-90 (black), b) SCM-6-90 (blue), c) SCM-6-500 (green), d) SCM-6-700 (orange), and e) SCM-6-800 (red).

treatment, and the growth of graphitic domains from this preorganized state. The 1,2-benzoquinone- and urea-based material (SCM-2-90) exhibits a well-defined diffraction patterns (Figure 2a), which confirms the presence of larger precursor crystals. These crystals are not the focus of the present manuscript, but serve as a low molecular weight model to provide some insights into the reaction mechanism. Materials synthesized with precursors having greater numbers of hydroxyl- or oxo-groups (SCM-4-135 Figure SI-5, Supporting Information and SCM-6-90 Figure 2b) exhibit broader peaks typical for noncrystalline polymers. The primary reflection observed for these materials is centered at ≈26° of 2θ, and is usually attributed to the stacking of aromatic systems.[30] Further, SCM-6-90 reveals a second broad reflection centered at around 14° which has been attributed to the in-plane ordering of the H-bridged complexes. This is supported by the ^{1}H solution-state NMR spectrum of SCM-6-90 which exhibits high intensity signals at positions between 10.5 and 12.0 ppm that are indicative of strong dipole-coupling between stacked and highly organized polarizable layers (Figure SI-6, Supporting Information) already in the liquid state. These aggregates can be also easily observed by AFM (data not shown here) where the sample appears to be composed of thin, primarily flake-like aggregates with thicknesses of ≈1 nm. Together, the presence of diffraction signals associated with aromaticity and intermolecular hydrogen bonding in the materials prior to high temperature treatment supports the unique degree of preorganization of the presented precursor system.

Heat treatment at elevated temperatures leads to X-ray diffractograms with more pronounced aromatic stacking peaks, typical of graphitic carbons, concurrent with development of the in-plane signal at ≈43°. This reflects the progressing condensation and extension of the aromatic system. The fast cross-linking at early reaction stages and the resulting high stability is supported by unusually high reaction yields (70–98 wt% and 10–30 wt% at low and high synthesis temperatures of 90 and 800 °C, respectively) as well as unusually high preservation of nitrogen content (Table 1). The outstanding value of 28 wt% nitrogen for the cyclohexanehexone- and urea-based material condensed at 800 °C (SCM-6-800) indicates that the initial nitrogen content can be preserved even at elevated temperatures. Note that the ideal "C_2N" would be characterized by 33 mol% of nitrogen that is indeed very close to the material even at the higher temperatures (Scheme 1). Retention of heteroatoms in general, and their presence in specific positions and moieties particularly, is highly desired since they are expected to introduce electronic structures which improve (electro)catalytic properties or performance in supercapacitor electrodes.[31] The unusually high retention if nitrogen also at elevated temperatures must be attributed to the initial preorganization of the precursors into aromatic systems at stable positions which do not require substantial rearrangement during heating. This is reflected also in the thermal development of the X-ray diffractograms of cyclohexanehexone-based materials (SCM-6-y) (Figure 2d–f), in which only minor changes in peak position and intensity are observed.

To identify the type of nitrogen in these materials, high-resolution nitrogen XPS was performed. Deconvolution of the N 1s peak according to electron binding energies established that SCM-6-500 and SCM-6-800 are primarily composed of pyridinic/pyrazinic and pyrrolic nitrogen species, as shown in **Table 2**. Graphitic (also referred to as "quaternary") nitrogen and nitroxide species are minority species in both materials, though their relative proportions increase at the higher condensation temperature. The high contents of nitrogen present in six-member aromatic rings such as pyridinic and/or pyrazinic moieties is very exciting, as the only way to incorporate such high quantities of nitrogen in such sites without C—H— bonds is in a structure similar to the one presented in Scheme 1. Although primarily composed of pyrazinic moieties, structural imperfections and nonclosed rings/surface termination are suspected as source of the 7 at% of pyrollic nitrogens. It is to be underlined that XPS is a surface sensitive technique, i.e., the 7 at% pyrrollic sites include the necessarily existing surface terminations, and the structural bulk content is presumably significantly higher. Here, it is noted that the solid-state NMR investigation of nitrogen-containing carbons is not trivial because of high electronic conductivity and has failed for similar systems in many cases. A more detailed investigation of the materials

Table 2. High-resolution N 1s XPS characterization of surface nitrogenous species of cyclohexanehexone- and urea-based materials (SCM-6-y) synthesized with 500 and 800 °C condensation temperatures including absolute and relative percentage of nitrogen in the material.

	Absolute and relative surface nitrogen species compositions at different condensation temperatures	
	500 °C	800 °C
Overall N	31.0 at% (100%)	22.5 at% (100%)
Pyrazinic/pyridinic N	20.7 at% (67%)	10.3 at% (46%)
Pyrrolic N	7.0 at% (23%)	6.0 at% (27%)
Graphitic N	2.4 at% (8 %)	4.1 at% (18%)
Nitroxide	0.9 at% (3%)	2.2 at% (10%)

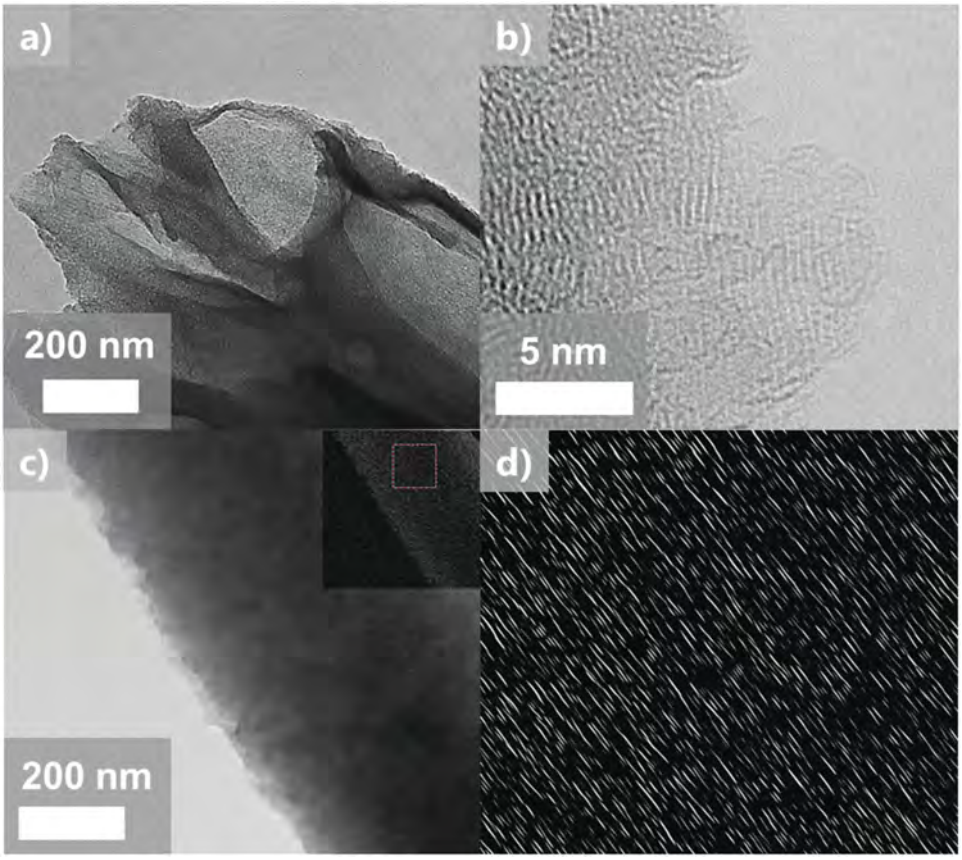

Figure 3. Transmission electron microscopy of morphosynthesis experiments with supramolecular carbonaceous materials based on cyclohexanehexone/urea to illustrate the structuring of the preorganized monomer mixtures: a) templated with SBA-15, "ordered mesoporous;" b–d) templated with $ZnCl_2$ salt melt for highly accessible micropores. b) Aberration correctedHR-TEM, c) overview image of region used for d) Fourier-filtered image (scale according to (c).

with this technique was performed and agrees with our structural models, though the data will be presented in all details in a following independent manuscript.

To demonstrate the versatility and processability of the SCM-approach not only to the level of molecular control of carbon ordering and heteroatom substitution patterns, also the micro- and nanoarchitecture of the materials was synthetically controlled toward different morphologies. Representatively performed with the cyclohexanehexone-based system, nanoarchitectures including ordered mesopores with high surface area and zeolite-like materials were obtained by using either SBA-15 as a hard template or salt templating/salt melt synthesis, respectively.[32] TEM images reveal that both templating methods can be successfully employed for the morphosynthesis of differently structured, highly porous, nitrogen-containing carbon materials. For the material produced with SBA-15 (SCM-6-800-SBA-15) even the typical negative-line pattern structure of the initial template is found (**Figure 3**a).

The presence of sufficiently thin morphologies also enables the application of aberration-corrected high-resolution transmission electron microscopy (HR-TEM) for characterization of the porous samples. Figure 3b–d shows a material prepared from cyclohexanehexone/urea at 700 °C in $ZnCl_2$ salt melt which is essentially composed of stacked but partially bent graphitic layers with the typical stacking distance of 0.35 nm, as already observed in the XRD experiments. The fact that the thicker grains are composed of lamellar substructures is visible in Figure 3b, but can be further elaborated by electron diffraction and Fourier-filtered reconstituted images (Figure 3c,d). Contrary to classical carbon nitride samples or ordinary amorphous carbons, the samples are highly stable under the electron beam.

Nitrogen sorption experiments further confirm the successful templating by SBA-15 mesostructured silica and $ZnCl_2$ salt to produce high surface area samples from this novel precursor system (**Figure 4**). Salt templating has turned out to be remarkably successful in the context of well-defined carbon structures.[10]

Specific surface area includes not only the outer structural surface, but also accessible meso- and micropores which contribute the majority of the surface area. The very high specific surface area of 1512 $m^2\ g^{-1}$ of the material prepared with $ZnCl_2$ salt together with the morphology observed in HR-TEM strongly hint to single carbon-nitrogen layers with densely packed zeolite-like pores. All data corroborate a structural model of porous layers where the pores are lined by pyrazinic nitrogens. The high surface areas together with the high nitrogen-functionality makes these materials of significant interest for (electro)catalytic applications.

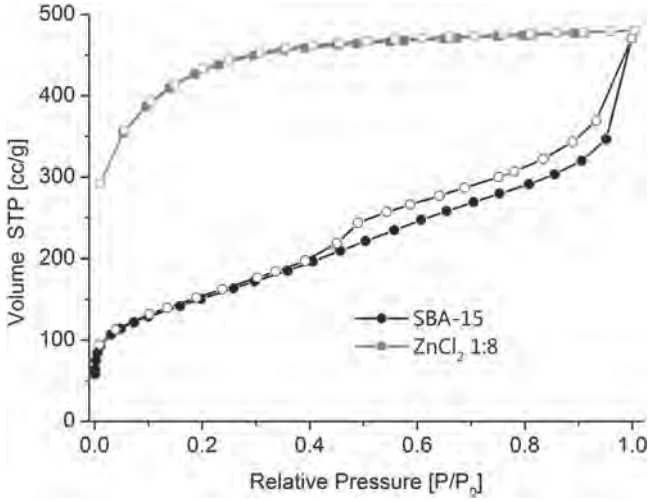

Figure 4. Nitrogen sorption isotherms of supramolecular carbonaceous materials based on cyclohexanehexone/urea templated with SBA-15 (synthesis at 800 °C, black circle) and $ZnCl_2$ (synthesis temperature 700 °C, red square). The solid symbols indicate adsorption branch, the open symbols, the desorption branch.

EELS was employed to examine the hybridization state around carbon and nitrogen (further elements including oxygen are not observed, **Figure 5** and Figure SI-7, Supporting Information).

A representative EELS spectrum recorded from the $ZnCl_2$-based sample over the energy range of the carbon K- and nitrogen K-edges is shown in Figure 5a. Both, the carbon K- and nitrogen N-edges show clear π^*- and σ^*-features, and from the integral intensity of the respective edges an elemental C/N ratio of roughly 80/20 can be estimated. The fine structure of the carbon K-edge reflects defective, sp^2-hybridized carbon with amorphous contributions. Compared to the carbon K-edge, the nitrogen edge shows more developed features in the π^*-region, reflecting differently coordinated N-species, a more pronounced valley between the π^*- and σ^*-features as well as a less broadened σ^*-feature, reflecting a higher degree of sp^2-ordering. The EELS fine structure contains information about the electronic structure at and in the surrounding of the ionized species. Hence, it can be assumed that the nitrogen atoms share the electronic structure with a portion of the carbon that is more ordered than what is reflected in the overall carbon K-edge. The excess of carbon that is found to be present by the EELS quantification therefore contributes to the amorphous portion of the carbon K-edge, while the nitrogen K-edge indicates that the special precursor bonding motif is kept throughout the condensation process. Overall, the EELS spectrum supports the suggested structural model of a slightly defective C_2N structure, as initially depicted in Scheme 1.

To illustrate the semi-metallic character of the carbon/nitrogen arrays synthesized by the present approach already at comparably low synthesis temperatures, conductivity measurements were performed on the non-templated SCM-6-800 synthesized at 800 °C. A value of 2 S cm^{-1} at 423 K was obtained for a sintered pellet, while Seebeck measurements clearly indicate the dominant *n*-character of the charge transport. The details of these electronic measurements however

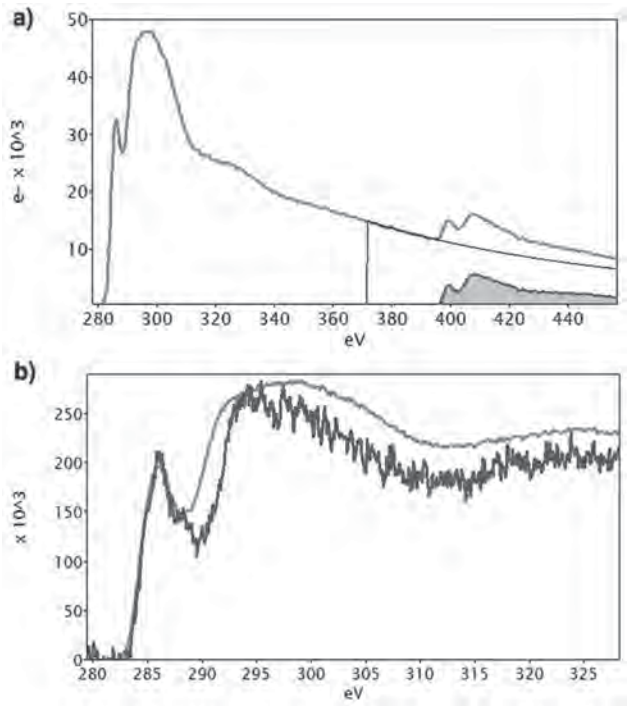

Figure 5. a) EELS of cyclohexanehexone/urea-based sample templated with $ZnCl_2$ showing the carbon K-edge (after background subtraction) as well as the N–K-edge (with and without background subtraction). b) Comparison of the fine structure of the respective edges. Although slightly more noisy, the spectral features are more developed in the N–K-edge, reflecting higher degree of structural ordering related with the local environment of the N-species.

exceed the limits of this publication and are subject to forthcoming work.

This article presents the use of a class of deep eutectic mixtures composed of oligophenol/ketones and urea to synthesize new carbon–nitrogen materials. The geometry of the phenol/ketone acts as a structure donating motif while the urea serves simultaneously as a melting point reduction agent and nitrogen source. As a specific example, materials generated from a mixture of cyclohexanehexone and urea were examined by elemental analysis, XRD, HR-TEM, EELS, and XPS. The data indicate that condensation of these two reactants occurs in a structurally organized fashion. Carbonaceous condensates with metallic gloss are obtained starting from reaction temperatures as low as 500 °C. The products condensed at 700–800 °C can be generally described as a disordered version of "C_2N" with a nitrogen content of 28 wt%, while the nitrogen is predominately placed in pyrazinic positions, with pyrollic nitrogens present for surface termination and as defect structures. HR-TEM analysis coupled with EELS gives indication for a locally highly organized lamellar structure, while determination of specific surface area on the same samples clearly shows that those lamellae must be microporous as such, that is the carbon sheets contain densely packed zeolithe-like pores which are lined with pyrazinic nitrogen. This represents a new structural paradigm in C/N-based materials, and it can be expected that the resulting family of N-modified carbons will effectively complement N-doped

carbons and carbon nitrides in their electronic, (electro)catalytic, and sorption applications.

Experimental Section

Synthesis: 1,2-dihydroxybenzene (Sigma–Aldrich, 105 °C decomposition), 2,5-dihydroxy-1,4-benzoquinone (Alfa Aesar, 220 °C sublimation), cyclohexanehexone octahydrate (Sigma–Aldrich, 99 °C decomposition), and urea (133 °C melting point) were used as received. To prepare 1,2-benzoquinone from 1,2-dihydroxybenzene, 0.5 g of 1 M NaOH solution was added to 5 g of 1,2-dihydroxybenzene under stirring and kept overnight to form dark blue crystals.

Mesostructured silica (SBA-15) was synthesized based on previously reported work.[33, 34] In brief, 8 g of poly(ethylene oxide)-poly(propylene oxide)-poly(ethylene oxide) triblock copolymer (Pluronic P123) was dissolved in 60 mL of deionized water. To this solution, 17 g of tetraethylorthosilicate and 240 mL of 3 M HCl were added, and vigorous stirring was performed for 10 min. Polymerization of the hydrolyzed silica precursors was accomplished by stirring the solution for 20 h at 40 °C. The solution was then held at 90 °C without stirring for 2 d, vacuum filtered, and calcined for 12 h at 550 °C to remove the triblock copolymer and produce the mesostructured silica powder.

In a typical "supramolecular carbon synthesis," stoichiometric amounts of the phenol/quinone and urea are mixed such that each oxogroup is paired by nitrogen-moiety of urea (i.e., 1,2-benzoquinone:urea in a 1:1 mole ratio, 2,5-dihydroxy-1,4-benzoquinone:urea 1:2 and cyclohexanehexone:urea 1:3). Deep eutectics were formed through gentle heating of the powder mixtures in a glass vial to temperatures between 90 and 135 °C depending on the specific precursor mixture. For the synthesis of the carbons, the eutectic mixtures were then heated to varying temperatures under nitrogen flow with a heating rate of 2.5 °C min^{-1} and held at the target temperature for 1 h.

Porous versions were produced from the precursor mixture containing a 1:3 mole ratio of cyclohexanehexone and urea using SBA-15 or $ZnCl_2$ as templates. For SBA-15, after heating the precursor mixture (1366 mg) at 90 °C to form a liquid, 1 mL of water (for reduced viscosity) is added, and the liquid was infiltrated under reduced pressure into 350 mg of SBA-15 powder. For the salt template, after heating the precursor mixture at 90 °C to form a liquid, the resolidified precursor mixture was ground at room temperature with $ZnCl_2$ in a weight ratio of precursor:salt of 1:8. After high-temperature heating (SBA-15 800 °C, $ZnCl_2$ 700 °C), the composite products were ground, with SBA-15 removed through stirring overnight in 250 mL of 1 M NaOH solution. $ZnCl_2$ salt was removed through washing in 1 L of water followed by washing in 1 M HCl. All products were finally dried in a vacuum oven at 50 °C.

The materials described herein are referenced as SCM-*x*-*y*, where SCM stands for supramolecular carbonaceous materials; *x* denotes the number of phenol/oxogroups of the educt, and *y* the synthesis condensation temperature.

Characterization: Bulk elemental composition was determined by combustion analysis using a Vario Micro device. Wide angle X-ray-patterns were taken on a Bruker D8 Advance instrument using Cu-K_α-radiation. Differential scanning calorimetry (DSC) was performed with a Mettler Toledo DSC 1 STARe System under nitrogen atmosphere. The samples were run in an aluminum crucible in a sealed furnace and heated to 200 °C with heating rate of 5 °C min^{-1}. Subsequently, the samples were cooled down at the same rate. Thermogravimetric analysis–mass spectrometry (TGA–MS) was performed using a Netsch thermogravimetry TG 209 F1 Libra linked to a Pfeiffer Vacuum Omnistar gas analysis system with 194 cycles 105 min^{-1} with detection in the range of M_w from 10 to 159 Da.

Transmission electron microscopy (TEM) images were obtained on a Zeiss EM 912Ω instrument and SEM images on a LEO 1550-Gemini instrument after sputtering with platinum. High-resolution TEM images and EELS spectra were recorded using a double Cs corrected JEOL ARM 200F instrument. Since the material demonstrated a very high stability against electron beam damage, the microscope was operated at 200 kV.

Nitrogen sorption measurements were performed using N_2 at 77 K after degassing the samples at 150 °C under vacuum for 20 h with a Quantachrome Quadrasorb SI porosimeter. The surface area was calculated by applying the Brunauer–Emmett–Teller model to the isotherm data points of the adsorption branch in the relative pressure range $p/p_0 < 0.3$ in the linear region with the best correlation. The pore size distribution was calculated from N_2 sorption data using the nonlocal density functional theory equilibrium model method for slit pores provided by Quantachrome data reduction software QuadraWin Version 5.05.

For AFM measurements, the initial concentration of liquid-crystalline eutectic mixture in the undercooled liquidus from cyclohexanehexone:urea mixture 1:3 (SCM-6-90) was diluted in water, thereafter drop-casted on a substrate (freshly cleaved mica), and left to dry at room temperature. AFM height and phase images were obtained in the soft tapping mode by Dimension 3100 AFM (Veeco/Bruker, USA) controlled by the Nanoscope IIIa controller (Digital Instruments/Bruker, USA). Standard silicone tips (Olympus, model OMCL-AC160TS, Japan; BudgetSensors, model Tap300-G, Bulgaria) with radius around 10 nm were used. Measurements were performed at room temperature, relative humidity of about 40%, in a low-noise acoustic chamber. For the evaluation of the AFM data Gwyddion 2.38 and NanoScope Analysis 1.50 were used.

Size exclusion chromatography (SEC) with simultaneous UV (270 nm) and RI detection was conducted in DMSO (+0.5 g L^{-1} LiBr) at 70 °C at a flow rate of 1.0 mL min^{-1} using a 50 mm × 7.5 mm and a 300 mm × 7.5 mm PSS-GRAL column (particle size, 10 µm; linear porosity, 500–1 × 10^6 g mol^{-1}). Solutions containing 1.5 g L^{-1} were filtered through 0.45 mm filters. The calibration was done with poly(methyl methacrylate) standards (PSS, Mainz, Germany).

Solution-state ^1H NMR spectroscopy was carried out at room temperature on a Bruker DPX-400 spectrometer operating at 400.1 MHz. Collected spectra consisted of the average of 10 000 scans collected with an acquisition time of 3.0 s. For the measurement, 20 mg of sample were dissolved in 0.7 mL of deuterated dimethyl sulfoxide (DMSO) and the solvent peak used for calibration.

Surface compositions of the materials were characterized by XPS using a Kratos Axis Ultra X-ray photoelectron spectroscopy system. These measurements characterized the elemental composition of the exterior 8–10 nm of sample particles with 0.1 at% resolution. Surface elemental compositions were determined using survey scans over a range of 1200 to 0 eV with a step size of 0.5 eV and a pass energy of 160 eV. Quantitative characterization of the presence of various nitrogenous sites was accomplished using high-resolution nitrogen XPS, scanning over a range of 413–390 eV with a step size of 0.05 eV and pass energy of 20 eV. Spectra were processed using CasaXPS software, and each distribution recorded by the high-resolution N scan was deconvoluted into multiple Gaussian line shapes based on the binding energies of electrons associated with nitrogens in various functional groups.[35]

Supporting Information

Supporting Information is available from the Wiley Online Library or from the author.

Acknowledgements

The work at UCSB was supported by the Institute for Collaborative Biotechnologies through Grant No. W911NF-0001 from the US Army Research Office. The content of the information does not necessarily reflect the position or the policy of the Government, and no official endorsement should be inferred. XPS characterization was conducted

at the MRL Shared Experimental Facilities, which are supported by the MRSEC program of the NSF under Award No. DMR 1121053; a member of the NSF-funded Materials Research Facilities Network (www.mrfn.org). The authors thank Guylhaine Clavel for HR-TEM measurements, Laurent Chabanne for TGA–MS measurements and Hubert Gojzewski and Rodrigo Pérez-García for AFM and Marlies Gräwert for GPC measurements. This work was partially supported by the IMI Program of the National Science Foundation under Award No. DMR 0843934, and the UCSB-MPG Program for International Exchange in Materials Science.

Received: March 30, 2015
Revised: June 8, 2015
Published online: July 14, 2015

[1] H.-P. Cong, J.-F. Chen, S.-H. Yu , *Chem. Soc. Rev.* **2014**, *43*, 7295.
[2] J. Liu, T. Yang, D.-W. Wang, G. Q. Lu, D. Zhao, S. Z. Qiao, *Nat. Commun.* **2013**, *4*, 2798.
[3] J. Liu, S. Z. Qiao, H. Liu, J. Chen, A. Orpe, D. Zhao, G. Q. Lu, *Angew. Chem. Int. Ed.* **2011**, *50* 5947.
[4] W. Li, Q. Yue, Y. Deng, D. Zhao, *Adv. Mater.* **2013**, *25*, 5129.
[5] A. Vu, X. Li, J. Phillips, A. Han, W. H. Smyrl, P. Bühlmann, A. Stein, *Chem. Mater.* **2013**, *25*, 4137.
[6] L. Zhao, L.-Z. Fan, M.-Q. Zhou, H. Guan, S. Qiao, M. Antonietti, M.-M. Titirici, *Adv. Mater.* **2010**, *22*, 5202.
[7] R. J. White, N. Brun, V. L. Budarin, J. H. Clark, M.-M. Titirici, *ChemSusChem.* **2014**, *7*, 670.
[8] J. P. Paraknowitsch, A. Thomas, *Macromol. Chem. Phys.* **2012**, *213*, 1132.
[9] J. S. Lee, X. Wang, H. Luo, S. Dai, *Adv. Mater.* **2010**, *22*, 1004.
[10] N. Fechler, T.-P. Fellinger, M. Antonietti, *Adv. Mater.* **2013**, *25*, 75.
[11] D. Carriazo, M. C. Serrano, M. C. Gutierrez, M. L. Ferrer, F. del Monte, *Chem. Soc. Rev.* **2012**, *41*, 4996.
[12] X. Zhu, P. C. Hillesheim, S. M. Mahurin, C. Wang, C. Tian, S. Brown, H. Luo, G. M. Veith, K. S. Han, E. W. Hagaman, H. Liu, S. Dai, *ChemSusChem* **2012**, *5*, 1912.
[13] J. P. Paraknowitsch, Y. Zhang, B. Wienerta, A. Thomas, *Chem. Commun.* **2013**, *49*, 1208.
[14] P. F. Fulvio, J. S. Lee, R. T. Mayes, X. Wang, S. M. Mahurina, S. Dai, *Phys. Chem. Chem. Phys.* **2011**, *13*, 13486.
[15] N. Fechler, T.-P. Fellinger, M. Antonietti, *J. Mater. Chem. A* **2013**, *1*, 14097.
[16] T.-P. Fellinger, D. S. Su, M. Engenhorst, De. Gautam, R. Schlögl, M. Antonietti, *J. Mater. Chem.* **2012**, *22*, 23996.
[17] W. Yang, T.-P. Fellinger, M. Antonietti, *J. Am. Chem. Soc.* **2011**, *133*, 206.
[18] J. Liang, Y. Jiao, M. Jaroniec, S. Z. Qiao, *Angew. Chem.* **2012**, *124*, 11664.
[19] Y. Jiao, Y. Zheng, M. Jaroniec, S. Z. Qiao, *J. Am. Chem. Soc.* **2014**, *136*, 4394.
[20] L.-F. Chen, Z.-H. Huang, H.-W. Liang, H.-L. Gao, S.-H. Yu, *Adv. Funct. Mater.* **2014**, *24*, 5104.
[21] D. S. Dhawale, G. P. Mane, S. Joseph, C. Anand, K. Ariga, A. Vinu, *Chem. Phys. Chem.* **2013**, *14*, 1563.
[22] A. Vinu, K. Ariga, T. Mori, T. Nakanishi, S. Hishita, D. Golberg, Y. Bando, *Adv. Mater.* **2005**, *17*, 1648.
[23] D. Carriazo, M. C. Gutiérrez, F. P. J. M. Rojo, J. L. G. Fierro, M. L. Ferrer, F. del Monte, *Chem SusChem* **2012**, *5*, 1405.
[24] N. López-Salas, M. C. Gutiérrez, C. O. Ania, J. L. G. Fierro, M. L. Ferrer, F. del Monte, *J. Mater. Chem. A* **2014**, *2*, 17387.
[25] J. Zakzeski, P. C. A. Bruijnincx, A. L. Jongerius, B. M. Weckhuysen, *Chem. Rev.* **2010**, *110*, 3552.
[26] V. Molinari, C. Giordano, M. Antonietti, D. Esposito, *J. Am. Chem. Soc.* **2014**, *136*, 1758.
[27] P. Ferrini, R. Rinaldi, *Angew. Chem. Int. Ed.* **2014**, *53*, 8634.
[28] B. Joffres, C. Lorentz, M. Vidalie, D. Laurenti, A.-A. Quoineaud, N. Charon, A. Daudin, A. Quignard, C. Geantet, *Appl. Catal. B: Environmental* **2014**, *145*, 167.
[29] K. Ariga, A. Vinu, Y. Yamauchi, Q. Ji, J. P. Hill, *Bull. Chem. Soc. Jpn.* **2012**, *85*, 1.
[30] K. P. Gierszal, M. Jaroniec, T.-W. Kim, J. Kim, R. Ryoo, *New J. Chem.* **2008**, *32*, 981.
[31] K. Jurewicz, K. Babeł, A. Źiółkowski, H. Wachowska, *Electrochim. Acta* **2003**, *48*, 1491.
[32] X. F. Liu, N. Fechler, M. Antonietti, *Chem. Soc. Rev.* **2013**, *42*, 8237.
[33] D. Zhao, J. Feng, Q. Huo, N. Melosh, G. H. Fredrickson, B. F. Chmelka, G. D. Stucky, *Science* **1998**, *279*, 548.
[34] D. Zhao, Q. Huo, J. Feng, B. F. Chmelka, G. D. Stucky, *J. Am. Chem. Soc.* **1998**, *120*, 6024.
[35] a) R. J. J. Jansen, H. van Bekkum, *Carbon* **1995**, *33*, 1021; b) A. Dorjgotov, J. Ok, Y. Jeon, S. H. Yoon, Y. G. Shul, *J. Appl. Electrochem.* **2013**, *43*, 387.

ADVANCED MATERIALS

Supporting Information

for *Adv. Mater.*, DOI: 10.1002/adma.201501503

Eutectic Syntheses of Graphitic Carbon with High Pyrazinic Nitrogen Content

Nina Fechler, Niels P. Zussblatt, Regina Rothe, Robert Schlögl, Marc-Georg Willinger, Bradley F. Chmelka, and Markus Antonietti*

Supporting Information

Eutectic Syntheses of Graphitic Carbon with high Pyrazinic Nitrogen Content

Nina Fechler [a]*, Niels P. Zussblatt [b], Regina Rothe [a], Robert Schlögl [c], Marc-Georg Willinger [c], Bradley F. Chmelka [b], and Markus Antonietti, [a]

[a] Max Planck Institute of Colloids and Interfaces, Department of Colloid Chemistry, Research Campus Golm, 14424 Potsdam, Germany

[b] University of California at Santa Barbara, Department of Chemical Engineering, Santa Barbara, California 93106, United States

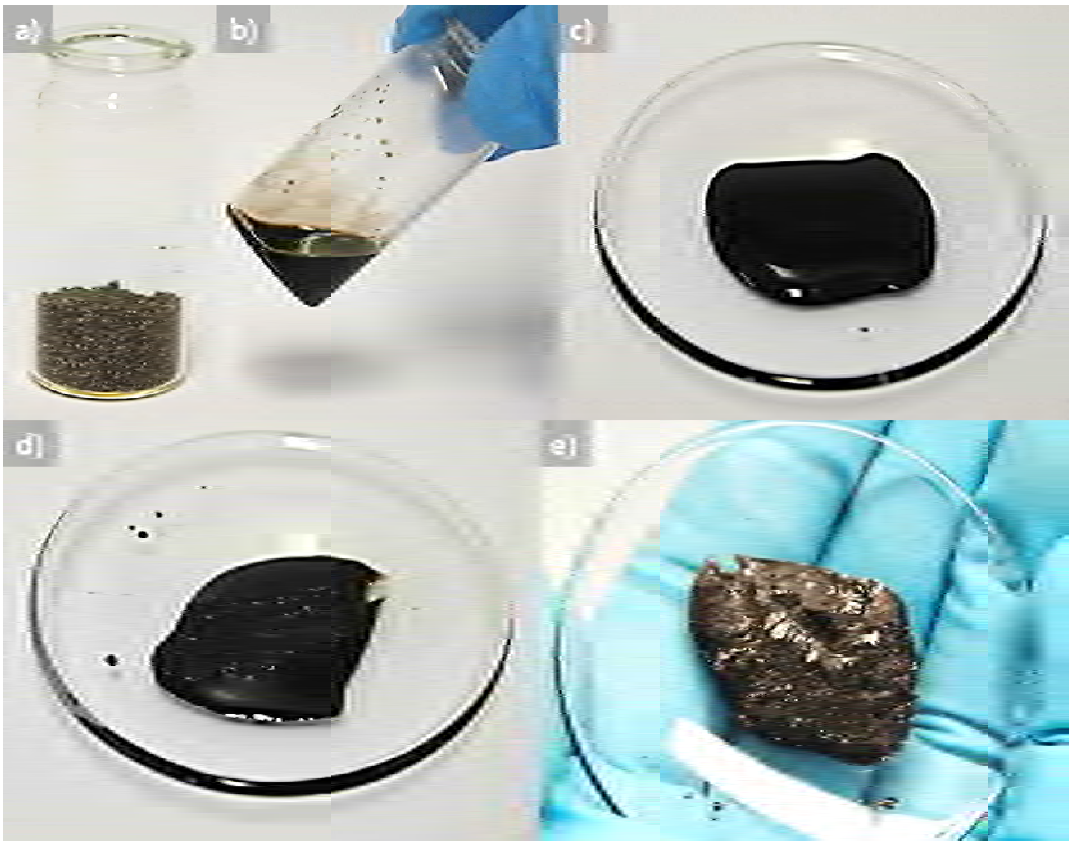

Figure SI-1: Photographs of the synthesis process of the 1,2-benzoquinone and urea based system (SCM-2-y): (a) powder of the 1,2-benzoquinone:urea mixture at room temperature, (b, c) powder-to-liquid transition at 90 °C (SCM-2-90), (d) onset of crystallization upon cooling back to room temperature finally resulting in a crystalline solid (e).

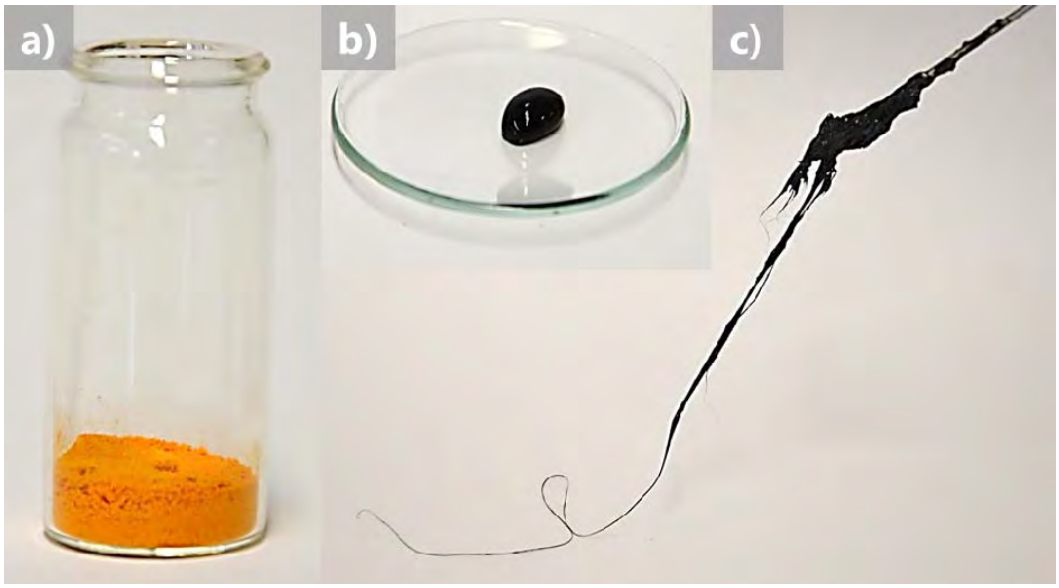

Figure SI-2: Photographs of the synthesis process of the 2,5-dihydroxy-1,4-benzoquinone and urea based system (SCM-4-y): (a) powder of the 2,5-dihydroxy-1,4-benzoquinone:urea mixture at room temperature, (b) powder-to-liquid transition at 135 °C (SCM-4-135), (c) plastic, processable intermediate.

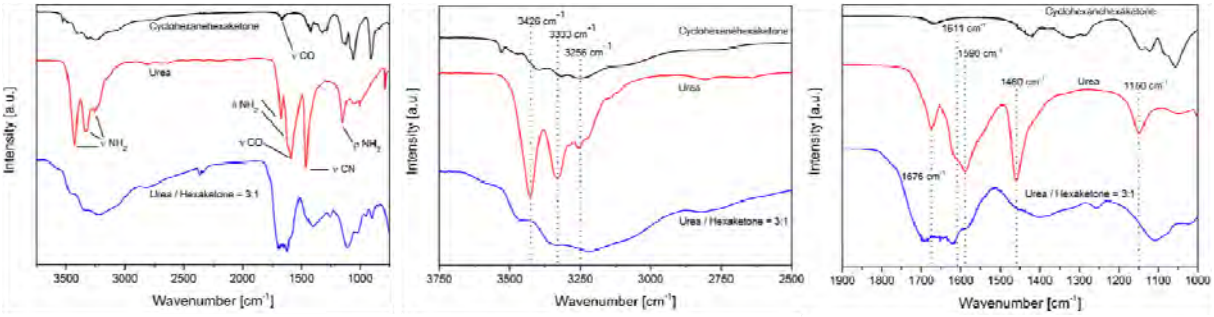

Figure SI-3: FT-IR-spectrum of urea, cyclohexanehexone and the solid urea/hexaketone mixture prepared at 90 °C, overview (left) and magnifications (middle and right).

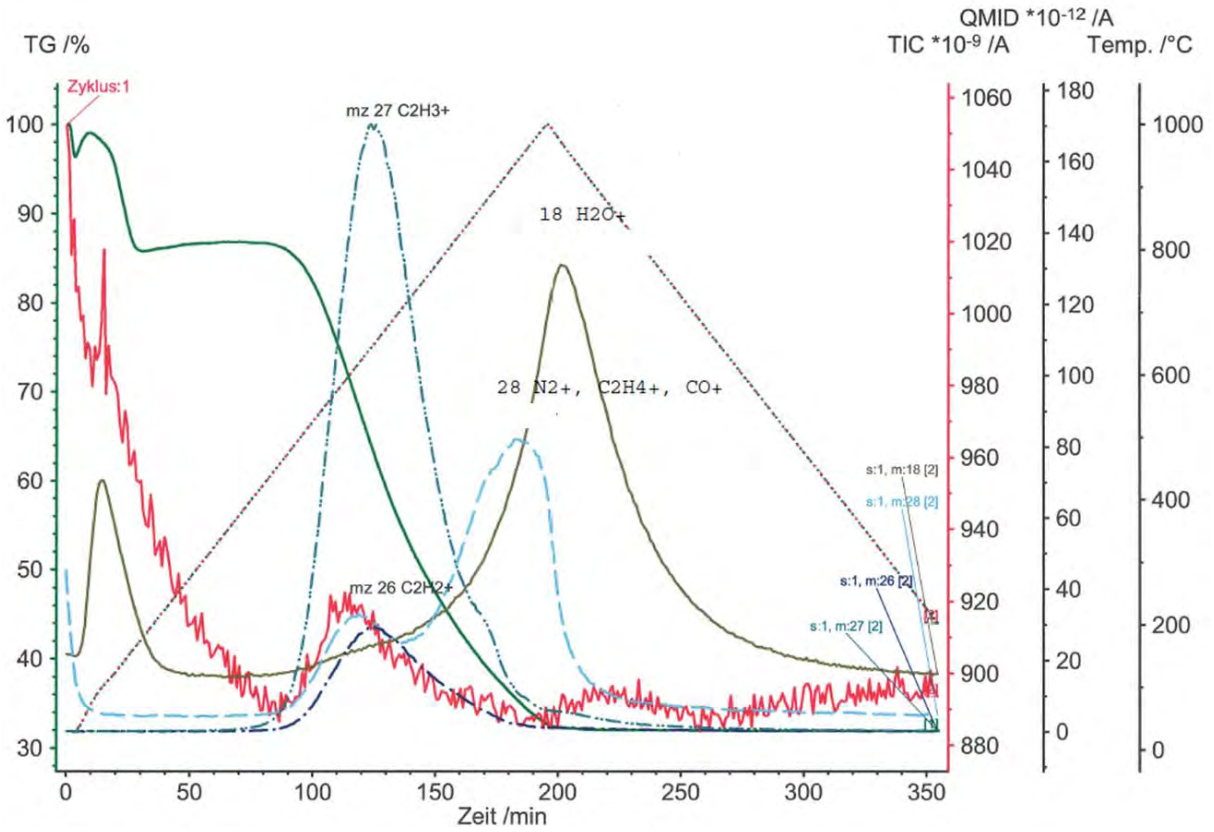

Figure SI-4: TGA-MS measurement of cyclohexanehexone and urea powder mixture.

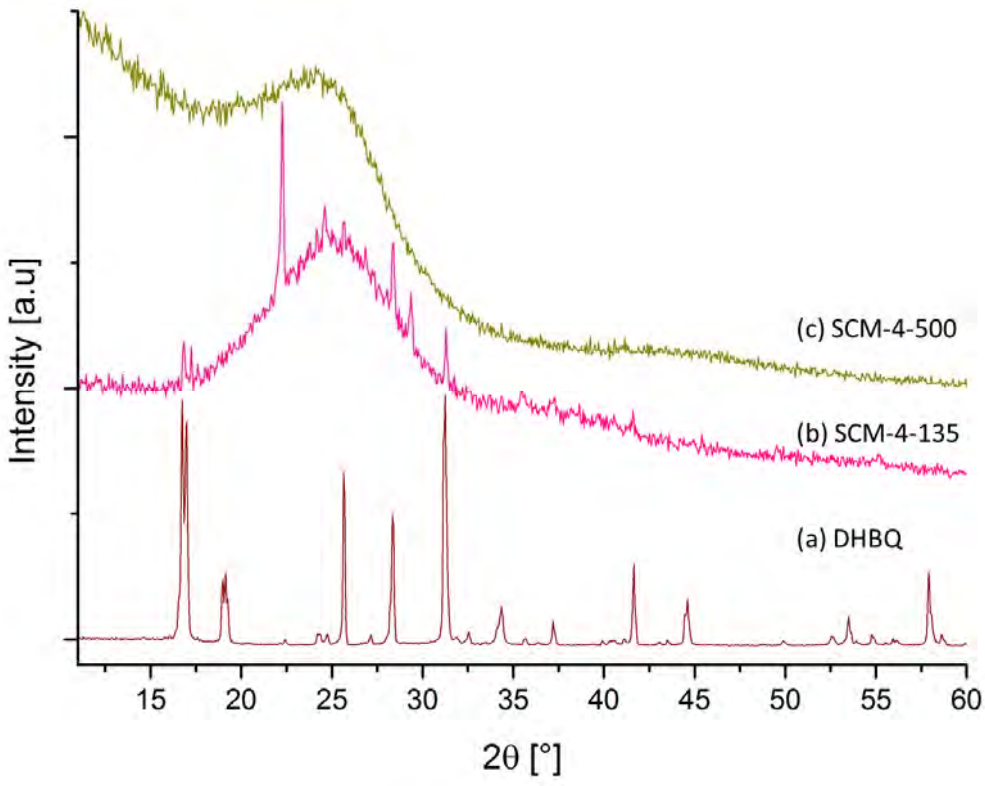

Figure SI-5. X-ray diffraction patterns of (a) 2,5-dihydroxy-1,4-benzoquinone (DHBQ, wine-red) and supramolecular carbonaceous materials based on 2,5-dihydroxy-1,4-benzoquinone at varying condensation temperatures (b) SCM-4-135 (pink), (c) SCM-4-500 (olive).

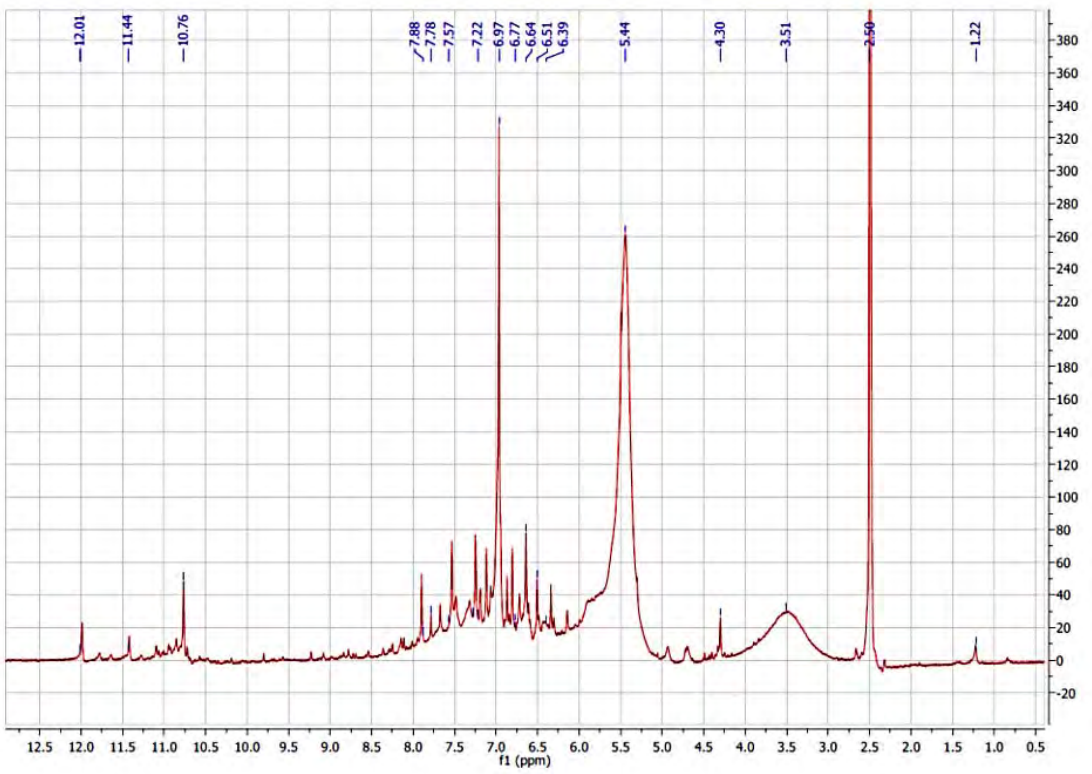

Figure SI-6. ^{1}H-NMR of cyclohexanehexone- and urea-derived material after 90 °C (SCM-6-90) in DMSO.

Table SI-1. X-ray photoelectron spectroscopy (XPS) surface elemental composition of cyclohexanehexone- and urea-derived materials (SCM-6-y) at various pyrolysis temperatures (y).

Condensation temperature (y) [°C]	*Surface elemental composition [atom%]*		
	C	N	O
90	46.9	19.0	34.1
500	63.7	31.0	5.3
800	73.3	22.5	4.1

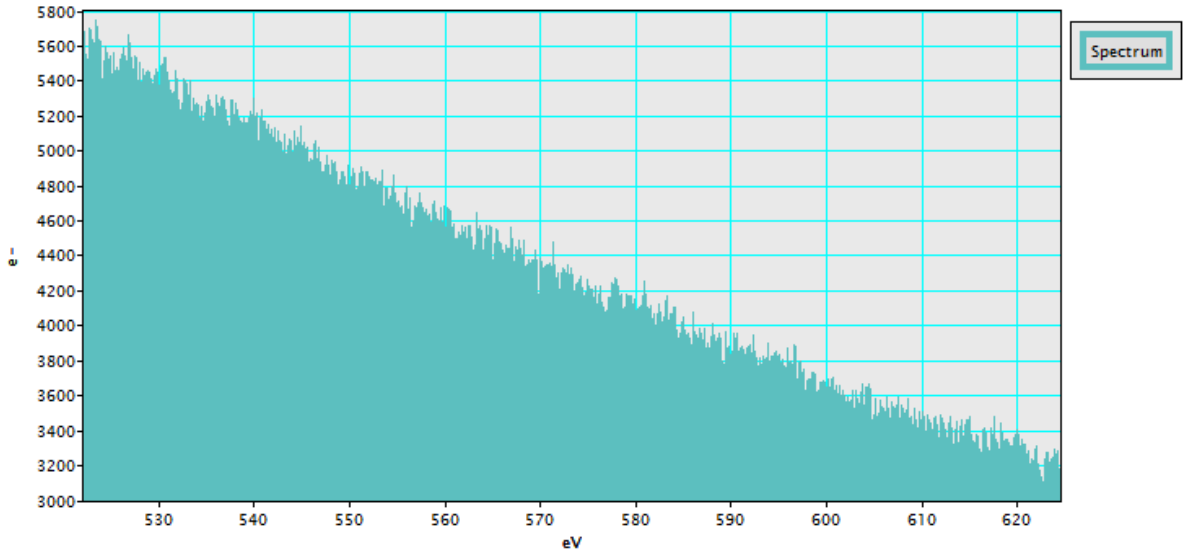

Figure SI-7. EELS of cyclohexanehexone/urea based sample templated with $ZnCl_2$ showing the region of O-K-edge.